Compact high-power optical source for resonant infrared pulsed laser ablation and deposition of polymer materials

V. Z. Kolev,[1] M. W. Duering,[1,2] B. Luther-Davies,[1] and A. V. Rode[1]

[1]*Laser Physics Centre, Research School of Physical Sciences and Engineering, The Australian National University, Canberra, Australian Capital Territory 0200, Australia*
vesselin.kolev@anu.edu.au

[2]*Fraunhofer-Institut für Lasertechnik ILT, Steinbachstr. 15, 52074 Aachen, Germany*

Abstract: We propose a novel tuneable table-top optical source as an alternative to the free electron laser currently used for resonant infrared pulsed laser deposition of polymers. It is based on two-stage pulsed optical parametric amplification using MgO doped periodically poled lithium niobate crystals. Gain in excess of 10^6 in the first stage and pump depletion of 58% in the second stage were achieved when the system was pumped by a high-power Nd:YVO_4 picosecond laser source at 1064 nm and seeded by a CW tuneable diode laser at 1530 nm. An average power of 2 W was generated at 3.5 μm corresponding to 1.3 μJ pulse energy.

OCIS codes: (190.4970) Parametric oscillators and amplifiers; (190.2620) Frequency conversion; (350.3390) Laser materials processing

References and links

1. D. M. Bubb, J. S. Horwitz, R. A. McGill, D. B. Chrisey, M. R. Papantonakis, R. F. Haglund, Jr., and B. Toftmann, "Resonant infrared pulsed-laser deposition of a sorbent chemoselective polymer," Appl. Phys. Lett. **79**, 2847-2849 (2001).
2. M. R. Papantonakis, and R. F. Haglund, Jr., "Picosecond pulsed laser deposition at high vibrational excitation density: the case of poly(tetrafluoroethylene)," Appl. Phys. A **79**, 1687-1694 (2004).
3. B. Toftmann, M. R. Papantonakis, R. C. Y. Auyeung, W. Kim, S. M. O'Malley, D. M. Bubb, J. S. Horwitz, J. Schou, P. M. Johansen, and R. F. Haglund, "UV and RIR matrix assisted pulsed laser deposition of organic MEH-PPV films," Thin Solid Films **453-454**, 177-181 (2004).
4. D. M. Bubb, J. S. Horwitz, J. H. Callahan, R. A. McGill, E. J. Houser, D. B. Chrisey, M. R. Papantonakis, R. F. Haglund, Jr., M. C. Galicia, and A. Vertes, "Resonant infrared pulsed-laser deposition of polymer films using a free-electron laser," J. Vac. Sci. Technol. A **19**, 2698-2702 (2001).
5. D. M. Bubb, M. R. Papantonakis, B. Toftmann, J. S. Horwitz, R. A. McGill, D. B. Chrisey, and R. F. Haglund, Jr., "Effect of ablation parameters on infrared pulsed laser deposition of poly(ethylene glycol) films," J. Appl. Phys. **91**, 9809-9814 (2002).
6. D. M. Bubb, B. Toftmann, R. F. Haglund, Jr., J. S. Horwitz, M. R. Papantonakis, R. A. McGill, P. W. Wu, and D. B. Chrisey, "Resonant infrared pulsed laser deposition of thin biodegradable polymer films," Appl. Phys. A **74**, 123-125 (2002).
7. B. Köhler, U. Bäder, A. Nebel, J.-P. Meyn, and R. Wallenstein, "A 9.5-W 82-MHz-repetition-rate picosecond optical parametric generator with cw diode laser injection seeding," Appl. Phys. B **75**, 31-34 (2002).
8. F. Brunner, E. Innerhofer, S. V. Marchese, T. Südmeyer, R. Paschotta, T. Usami, H. Ito, S. Kurimura, K. Kitamura, G. Arisholm, and U. Keller, "Powerful red-green-blue laser source pumped with a mode-locked thin disk laser," Opt. Lett. **29**, 1921-1923 (2004).
9. E. Innerhofer, F. Brunner, S. V. Marchese, R. Paschotta, G. Arisholm, S. Kurimura, K. Kitamura, T. Usami, H. Ito, and U. Keller, "Analysis of nonlinear wavelength conversion system for a red-green-blue laser-projection source," J. Opt. Soc. Am. B **23**, 265-275 (2006).
10. G. Arisholm, R. Paschotta, and T. Südmeyer, "Limits to the power scalability of high-gain optical parametric amplifiers," J. Opt. Soc. Am. B **21**, 578-590 (2004).
11. B. Luther-Davies, V. Z. Kolev, M. J. Lederer, N. R. Madsen, A. V. Rode, J. Giesekus, K.-M. Du, and M. Duering, "Table-top 50-W laser system for ultra-fast laser ablation," Appl. Phys. A **79**, 1051-1055 (2004).

#74496 - $15.00 USD Received 28 August 2006; revised 2 December 2006; accepted 2 December 2006

12. V. Z. Kolev, M. J. Lederer, B. Luther-Davies, and A. V. Rode, "Passive mode locking of a Nd:YVO_4 laser with an extra-long optical resonator," Opt. Lett. **28**, 1275-1277 (2003).
13. H. Ishizuki, and T. Taira, "High-energy quasi-phase-matched optical parametric oscillation in a periodically poled MgO:$LiNbO_3$ device with a 5 mm × 5 mm aperture," Opt. Lett. **30**, 2918-2920 (2005).
14. R. L. Sutherland, *Handbook of nonlinear optics* (Marcel Dekker, 1996).
15. SNLO nonlinear optics code available from A. V. Smith, Sandia National Laboratories, Albuquerque, NM 87185-1423.
16. I. Shoji, T. Kondo, A. Kitamoto, M. Shirane, and R. Ito, "Absolute scale of second-order nonlinear-optical coefficients," J. Opt. Soc. Am. B **14**, 2268-2294 (1997).
17. R. C. Miller, "Optical second harmonic generation in piezoelectric crystals," Appl. Phys. Lett. **5**, 17-19 (1964).

1. Introduction

Thin polymer films are widely used for a range of applications in conventional electronics, organic electronics and organic optoelectronics, photonics, sensor technology, medicine, etc. Currently, several different techniques exist for depositing polymer films (including chemical and solvent-based methods, physical vapour deposition, etc.) each with their own strengths and weaknesses. Resonant Infrared Pulsed Laser Deposition (RIR-PLD) [1] is a promising new approach for vacuum-phase deposition of polymers and organic molecules. As a dry, conformal, clean and environmentally friendly technique for producing organic films, it avoids a host of problems caused by solvents associated with commonly used spin- or dip-coating methods including solvent incompatibility, thickness control, and environmental contamination. The method employs a pulsed mid infrared laser source with a wavelength tuned to one of the molecular vibrational bands of the organic molecule to be ablated. Hence, the energy absorption can still be strong enough to localize energy deposition within a thin surface layer as required for laser ablation, but this leads to vibrational rather than electronic excitation of the target material, therefore, little chemical alteration or changes in the molecular weight distribution occur during the deposition. RIR-PLD has been successfully employed to deposition of a variety of technologically important polymers with applications ranging from micro-electro-mechanical systems (MEMS) [2], biological and chemical sensors [1], and photonics [3] to biocompatible medical-device coatings [4,5] and biodegradable time-release drug-delivery encapsulation [6].

In all these experiments a free electron laser (FEL) was used as an optical source for RIR-PLD, most often tuned to the C-H or O-H stretch vibrational bands around 3.4 μm and 2.9 μm, respectively. FELs provide widely tuneable high repetition rate trains of intense picosecond pulses, however they are large (building sized) and expensive facilities. For RIR-PLD to become a technologically useful technique table-top laser sources are required.

Whilst the physical mechanisms involved in RIR-PLD are not well understood, a number of key laser parameters appear to be important for successful implementation of the technique. These include: laser pulse durations in the picosecond range; single pulse energies around 1 μJ; and pulse repetition periods much shorter than cooling time of the laser-heated layer (100 μs – 1 ms). Experiments with the FEL have also shown that average powers of a few Watts are adequate for polymer ablation. Here we propose a tuneable table-top laser source achieving these parameters based on dual-stage optical parametric amplifier (OPA) and designed to excite the C-H stretch molecular absorption band present in most polymer materials. The advantage of this design is that it is technically straightforward and can be readily implemented using one of several commercially available picosecond Nd lasers. Compared with the alternative approach of using a synchronously pumped optical parametric oscillator, the OPA works with arbitrary pulse repetition rate; is simpler because it lacks any resonant cavity; is more easily tuned; and produces higher pulse energies. At the same time it provides excellent beam quality and good efficiency.

Using different nonlinear crystals the OPA technique has been successfully applied for various high average power applications [7-9] although at significantly lower pump and output pulse energies than reported here.

#74496 - $15.00 USD Received 28 August 2006; revised 2 December 2006; accepted 2 December 2006

2. System description

A schematic of the OPA is shown in Fig. 1. It consists of two amplifier stages: the first, a pre-amplifier operated at relatively low input power, high parametric gain and limited conversion efficiency (25-30%); and the second, a power amplifier pumped with high pulse power; relatively low parametric gain and higher efficiency (≈ 58%). This configuration overcomes the problem of degradation of the beam (and pulse) quality that occurs in single stage high-gain parametric amplifiers operated at high conversion efficiency due to reconversion of the generated waves back into the pump [10].

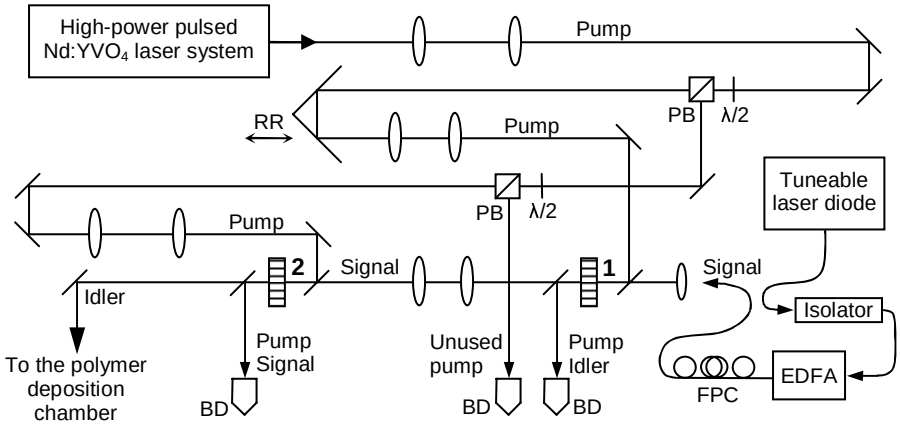

Fig. 1. Schematic drawing of the OPA system layout. Numbers 1 and 2 denote the two OPA stages using multiple-grating MgO:PPLN crystals mounted in temperature-controlled ovens. Abbreviations: PB – polarizing beam-splitter; λ/2 – half-wave plate; RR – retro-reflector; BD – beam dump; FPC – fiber polarization control.

The pump beam at 1064 nm was produced by a Master-Oscillator Power Amplifier (MOPA) system [11] consisting of a long-cavity passively mode-locked Nd:YVO_4 laser oscillator [12] coupled to a high-power folded single-pass Nd:YVO_4 amplifier, capable of producing average power in excess of 45 W. To pump the OPA, the oscillator was set to operate at 1.5 MHz repetition rate thus producing single pulse energies of up to 30 μJ. The pump pulses were measured to be ≈ 18 ps using a Femtochrome Research FX-103 autocorrelator. Combinations of a half-wave plate and a polarizing cube beam-splitter were used to adjust the required pump power for the first and the second stages of the optical parametric amplifier. In the experiments reported here only about 18 W of total average power was used. The maximum pump pulse energy for the second stage was 10 μJ. The two-lens telescopes used in the pump and seeding beam paths provided means for optimizing the beams sizes.

The first (high-gain) stage of the OPA was seeded with a continuous wave (CW) beam, produced by a tuneable external cavity diode laser source (TUNICS-Purity, Photonetics, Inc.) coupled to an erbium doped fiber amplifier (EDFA) (model AEDFA-LP, Amonics Ltd.). The maximum available seeding power was about 25 mW near 1530 nm. This arrangement provides a convenient alternative to the normal practice of seeding OPAs using parametric fluorescence from a high-gain optical parametric generator. The seed beam was delivered to the pre-amplifier using a single mode optical fiber via a pair of optical isolators and a polarization controller. Since the power per unit bandwidth of the seed beam significantly exceeded the optical parametric fluorescence from the pre-amplifier, the output spectrum of the pre-amplifier was determined solely by the operating frequency of the seed laser convolved with the time-dependent gain induced by the pump pulses in the OPA. As will be shown later, the OPAs have sufficient bandwidth that the idler output can be tuned over a

#74496 - $15.00 USD Received 28 August 2006; revised 2 December 2006; accepted 2 December 2006

range of around 35 nm by simply tuning the seed wavelength allowing the system to be tuned accurately to the maximum of the absorption bands of the polymer without any adjustment of the crystals.

After the first stage, the idler beam and unconverted pump were discarded, and the amplified pulsed signal beam was used to seed the second (high-power) parametric amplifier. A variable delay line incorporating a retro-reflector was used in the pump beam path for the first stage, leading to a controllable timing of the seeding pulses with respect to the pump pulses for the second stage so that a good temporal overlap could be achieved. After the second stage, the signal and the unconverted pump were discarded using a dichroic mirror leaving the remaining mid infrared idler as the output beam of the source.

Due to its high nonlinearity and wide quasi-phase-matching range achievable using periodic poling, lithium niobate (PPLN) was chosen as the nonlinear medium. Another advantage of PPLN is the maturity of its production technology. Hence, high-quality large-aperture crystals are becoming commercially available, allowing convenient power scalability through increasing the beam sizes. Periodically poled crystals with apertures as large as 5 mm × 5 mm have been recently reported for high-energy applications [13]. Doping with MgO (5 mol %) is usually used to improve resistance to photo-refractive damage and to reduce the coercive field required for periodic poling. In our setup, the two OPA stages used two identical 10 mm long MgO doped periodically poled lithium niobate (MgO:PPLN) crystals. Every crystal had six regions with different poling periods, each region with a cross-section of 2 mm × 2 mm. To further increase the photorefractive damage threshold and for fine wavelength tuning, the crystals were mounted in ovens and operated at elevated temperatures controllable within 100-200°C with an accuracy of 0.1°C. A set of appropriate grating periods (29.37 μm, 29.60 μm, 29.86 μm, 30.13 μm, 30.46 μm, and 30.84 μm) was chosen so that the temperature tuning ranges of neighboring gratings overlapped. Therefore, the seed signal beam could be continuously tuned over a sufficient range to produce idler wavelengths anywhere in the 3.25-3.6 μm band allowing precise tuning to the C-H stretch absorption bands of a wide range of different polymers.

3. Performance of the first stage

The purpose of the pre-amplifier stage was to provide a good quality pulsed seed beam for the power amplifier. All results reported in this paper were obtained using the gratings with period of 29.86 μm operated at about 145°C which corresponded to peak gain at 1530 nm for the signal and a corresponding idler wavelength of 3.5 μm. As shown in Fig. 2, a high gain in excess of 10^6 and a pump depletion of more than 40% could be achieved in the first stage OPA using a 2-3 W pump beam with a cross-section 140 μm × 115 μm and a seeding beam with diameter of 185 μm ($1/e^2$ intensity used throughout the paper, unless stated otherwise).

Since near diffraction limited beams were required from the OPA, the value of M^2 for the signal beam at the output of the first stage was measured as a function of the pump depletion [see Fig. 2(b)]. It is important to note that the output signal of the first stage consisted of two distinct beams which had different propagation parameters – the amplified pulsed beam whose propagation properties were modified by strong amplification by the pump and the residual CW seed beam between the pump pulses which was essentially unchanged after passing through the crystal. Because the duty cycle of the amplified signal pulses was small (2×10^{-5}) at low gain the average powers of the two beams after the first stage could be comparable and this led to an apparent increase of M^2 for the signal beam at low pump depletion. On the other hand the deterioration of beam quality at high pump depletion levels (> 35%) was due to reconversion of the signal and idler beam into the pump which occurred preferentially on the beam axis where the intensity was highest, that is where the parametric interaction was strongest. Since reconversion is very sensitive to pump intensity which varies across the beam (and pulse), it results in beam (and pulse) distortion. From Fig. 2(b), the optimal regime of operation of this first stage was at about 30% pump depletion corresponding to acceptable conversion efficiency and good beam quality: $M^2 < 1.25$. The slightly higher values of M^2 recorded for the horizontal direction reflected the poorer value of

#74496 - $15.00 USD Received 28 August 2006; revised 2 December 2006; accepted 2 December 2006

M^2 along the horizontal axis characteristic of the pump beam which was an inherent feature of the high-power amplifier used in the pump laser system.

Pulse shortening can be expected in high gain pre-amplifiers due to the time dependent gain during the pulse. The output pulse duration was measured using an autocorrelator based on two-photon absorption in a silicon p-i-n photodiode. The duration of the signal pulses was found to be in the range of 10-12 ps. Measurements of the output spectrum using an ANDO optical spectrum analyzer demonstrated that the pulses were close to transform limited.

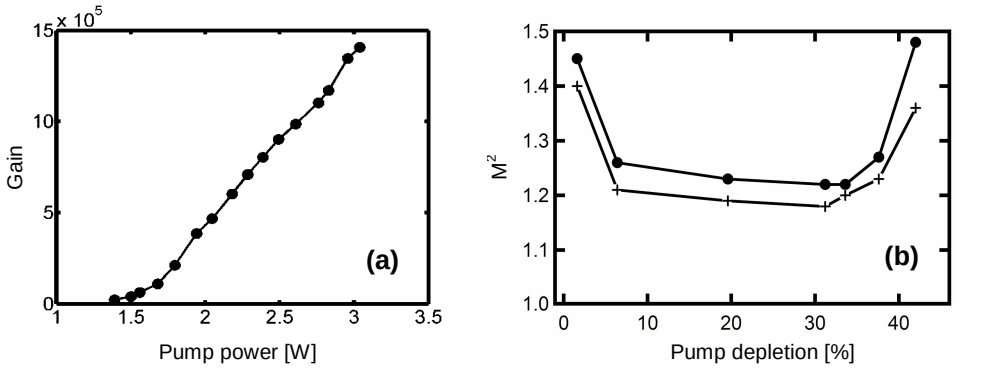

Fig. 2. (a) Gain versus pump power in the first stage OPA; (b) M^2 of the amplified in the first stage signal beam in horizontal (dots) and vertical (crosses) directions at different levels of pump depletion.

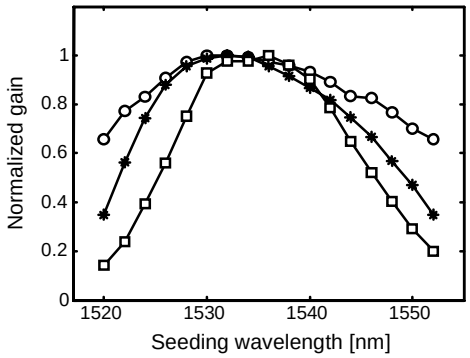

Fig. 3. Normalized gain as a function of seeding wavelength at constant seeding power and crystal temperature. The three curves correspond to different pump power levels in the order of 2 W (squares), 2.5 W (stars), and 3 W (circles).

A significant advantage of using OPAs for frequency conversion is their convenient tuning characteristics. It is well known (see e.g. [14]) that the sensitivity of gain to phase mismatch in the nonlinear crystal is reduced in conditions of high gain. This is demonstrated in Fig. 3 where we plot the normalized gain of the first stage as a function of seed laser wavelength. During these experiments the crystal temperature was kept constant at 143°C and the seed power was also held constant by adjusting the gain of the EDFA. The gain bandwidth was significantly higher than that resulting from phase mismatching at low gain [14], and further increased with higher pump power (i.e. higher gain). At highest gain the signal wavelength could be tuned over 25 nm with only a 20% reduction in output power (corresponding to about 35 nm of idler tuning).

#74496 - $15.00 USD Received 28 August 2006; revised 2 December 2006; accepted 2 December 2006

4. Optimization of the second stage

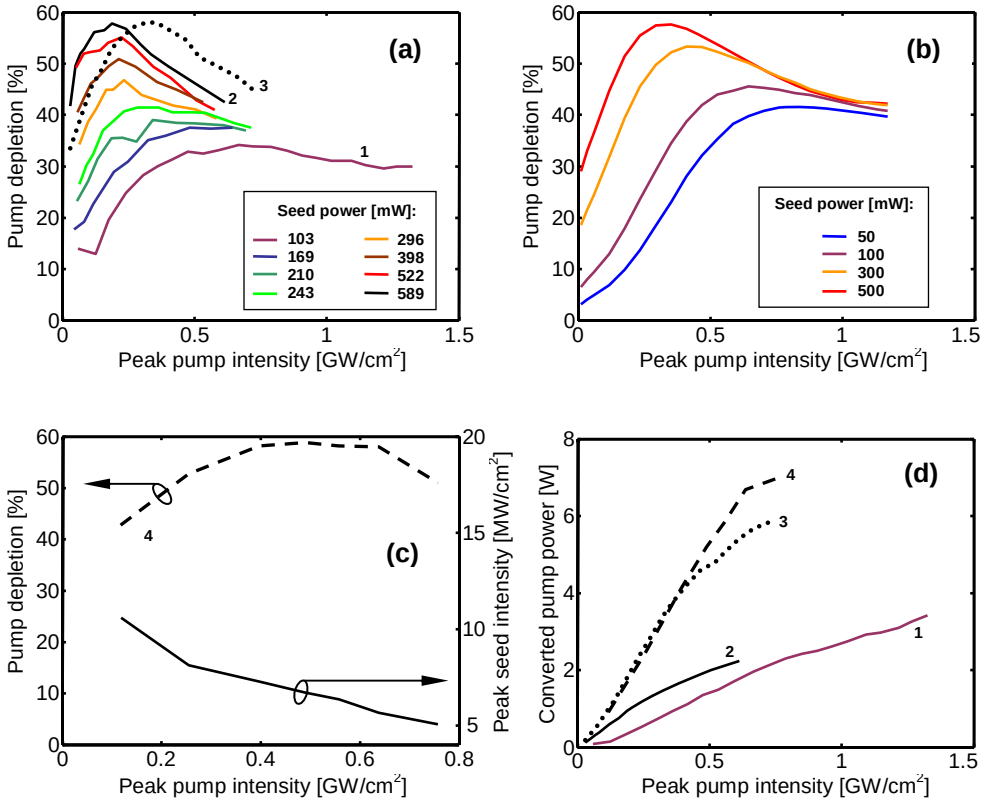

Fig. 4. Performance optimization of the second stage OPA: (a) Pump depletion as a function of peak pump intensity at different seed power; w_{pump} = 140 µm (solid curves); w_{pump} = 200 µm (dotted curve). (b) Theoretical results using w_{pump} = 140 µm and w_{seed} = 415 µm. (c) Optimised performance (dashed curve) via varying seed intensity (solid curve) at each pump intensity; all other parameters are the same as for Curve 3. (d) Converted pump power versus peak pump intensity; throughout the figure, curves with identical numbers represent the same data sets.

The purpose of the second (high power) OPA stage was to amplify the ≈ 0.5 W average power signal pulses from the first stage to generate a few watts of average power in the idler beam, thus around 5 W of signal output was required corresponding to a large signal gain in the order of 10. Therefore, the gain in the second stage was much lower than the first stage, but the average power levels were considerably higher. We characterized the dependence of the pump depletion on the peak pump intensity and this is shown in Fig. 4(a). Each of the solid curves corresponds to a different seed power, obtained by changing the pump power in the pre-amplifier stage, increasing from 103 mW (Curve 1) to 589 mW (Curve 2). For these data the Gaussian pump beam radius was 140 µm but the signal beam radius and overlap with the pump beam was optimised at low pump intensity (≈ 0.1 GW/cm^2) at each seed power. The seed beam radius thus varied in the range of 340-420 µm (the smaller beams corresponded to lower seed powers). The pump power was then varied and the corresponding pump depletion determined. As it can be seen from Fig. 4(a), pump depletion gradually increased with pump intensity until it reached a maximum, and then decreased due to increasing reconversion. The maximum conversion efficiency corresponding to pump depletion of 58% was achieved at pump intensity close to 0.2 GW/cm^2 using the maximum seed power. Reducing the seed power led to decrease in the maximum achievable pump depletion and a shift in the position

#74496 - $15.00 USD Received 28 August 2006; revised 2 December 2006; accepted 2 December 2006

of the peak towards higher pump intensity. This reflects the fact that low seed power required higher gain in the second stage and hence higher pump intensity. In such conditions however reconversion of signal and idler beams into the pump becomes more serious, limiting the maximum conversion efficiency.

Simplified theoretical calculations were performed using the 2D-mix-LP model of SNLO code [15] for comparison with the experiments and the results are presented in Fig. 4(b). For these calculations the radius of the seed beam was fixed at 415 μm and the pump at 140 μm. The effective nonlinearity of the crystals had to be adjusted to 9.1 pm/V to obtain the measured conversion efficiencies. This somewhat lower value in comparison with the value of 11.3-13.2 pm/V, that could be derived form the published data [16] using Miller's rule [17], appeared to be due to irregularities in the poling of our thick crystals visible under an optical microscope. In our calculations we did not take into account the small variations in the seed beam properties which were present in the experiments as a result of changes in the gain guiding characteristics of the preamplifier as the pump power to this stage was varied to change the preamplifier output power. Nevertheless, the model predictions reproduced the measured behaviour of the second stage OPA very well and confirmed that optimum conversion requires a combination of high seed power from the preamplifier and low second stage gain. Higher gains (i.e. higher pump intensity) resulted in increasing reconversion which reduced the pump depletion and hence conversion efficiency.

Obviously it would be useful to shift the position of the maximum pump depletion towards higher pump intensities to create high power without the beam quality being degraded by reconversion. One way of achieving this is to increase the size of the pump beam as is demonstrated by the dotted Curve 3 in Fig. 4(a). By increasing the pump beam size by a factor of 1.43 the position of the maximum could be shifted to higher pump intensity (0.35 GW/cm^2) whilst maintaining high pump depletion (the seed power was held at its maximum value of 589 mW, i.e. the same as for Curve 2).

Further optimization was made by adjusting the seed beam intensity (via the seed beam size) at each pump intensity. The result is shown in the dashed Curve 4 in Fig. 4(c) whilst all other parameters remained the same as for Curve 3 in Fig. 4(a). The solid curve in the Fig. 4(c) shows that the corresponding seed intensity had to be gradually reduced (for a fixed seed power of 589 mW) as the pump intensity increased in order to get the highest conversion efficiency. Thus, we were able to further shift the maximum of the curve to pump intensities as high as 0.5-0.6 GW/cm^2 whilst maintaining the pump depletion at around 58%.

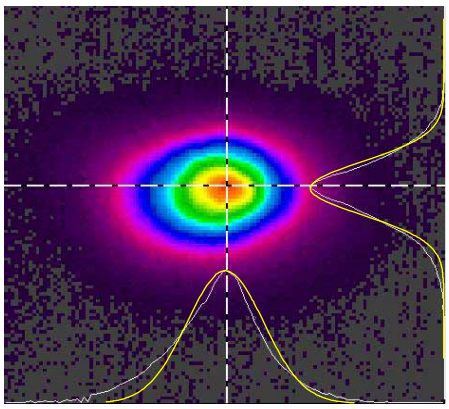

Fig. 5. Intensity distribution of the collimated output (idler) beam of the system at maximum output power. Gaussian fits to the intensity profiles are shown in yellow.

#74496 - $15.00 USD Received 28 August 2006; revised 2 December 2006; accepted 2 December 2006

It should be noted that although the fractional pump depletion in Fig. 4(a, c) displayed a maximum, the converted pump power always increases monotonically with increasing pump intensity as shown in Fig. 4(d). Here, Curves 1 to 4 represent data from the equivalent Curves 1 to 3 from Fig. 4(a) and Curve 4 from Fig. 4(c). The maximum converted pump power of ≈ 7 W was achieved at 0.75 GW/cm^2 and this corresponds to more than 2 W of mid infrared idler power at 3.5 μm. This was done at the point where some reconversion occurs which could affect the quality of the output beam. Nevertheless, the intensity distribution of the collimated output (idler) beam after the amplifier crystal determined using a Spiricon Pyrocam III camera was a good fit to a Gaussian profile as shown on Fig. 5. The slight asymmetry evident in horizontal direction is due to the slight asymmetry in the pump beam as discussed earlier.

To verify this power level was sufficient for polymer ablation we re-tuned the OPA to 3.38 μm corresponding to the C-H stretch of poly(methyl methacrylate) (PMMA). The beam was then passed via a Cambridge Technologies 2-D mirror scanner to a 200 mm focal length calcium fluoride lens that focused the beam to a spot of diameter of ≈ 85 μm (FWHM) onto a sample of PMMA in air. The beam was found to readily ablate the material for scanning speeds around 1 m/s. More precise measurements of the polymer ablation behaviour will be the subject of further research.

5. Conclusion and further development

We have demonstrated a compact table-top mid infrared optical source for RIR-PLD based on dual-stage OPA. A gain in excess of 10^6 was achieved in the first stage; the maximum conversion efficiency in the second stage reached 58%. The system was pumped by a pulsed (1.5 MHz repetition rate) Nd:YVO_4 MOPA system and seeded by a CW tuneable diode laser. An average power of 2 W, corresponding to a pulse energy of 1.3 μJ, was generated at 3.5 μm using multiple-grating MgO doped PPLN crystals.

This configuration could now be readily implemented using as a pump laser one of the several 10 W high repetition rate (> 500 kHz) Neodymium lasers commercially available from companies such as Time-bandwidth Products (Duetto) Lumera Laser GmbH (Staccato) or High-Q Laser GmbH (picoRegen). With careful optimization > 1.5 W of average power in the 3.5 μm band should be available from these systems which appears adequate for polymer ablation.

The fact that the maximum pump depletion in the second stage did not saturate at the maximum available seed power suggests that a further increase in the seed power to the second amplifier would result in higher conversion efficiency. This would allow further defocusing of the pump beam in the power amplifier and higher output power. To increase the overall efficiency of the system, another interesting solution is currently under development. The OPA configuration allows the unused signal output from the OPA to be converted into idler by placing an appropriate crystal immediately after the output of the second stage OPA. In this way we expect to increase the idler output power by 50% and our preliminary tests show very encouraging results.

Acknowledgements

The authors wish to thank Richard Haglund from Vanderbilt University, Nashville, TN for the fruitful discussions. The image on Fig. 5 was acquired using a Pyrocam III kindly lent by Spiricon, Inc. via their representative Brett Delahunty from Warsash Scientific Pty Ltd. The assistance of the Australian Research Council through its Federation Fellow and Linkage Grant programs is gratefully acknowledged.

#74496 - $15.00 USD Received 28 August 2006; revised 2 December 2006; accepted 2 December 2006